# Anthropogenic Influence on the 2021 Wettest September in Northern China

Ting Hu,[a] Ying Sun,[a,b] Xuebin Zhang,[c] Dongqian Wang,[a]

[a] *National Climate Center, Laboratory for Climate Studies, China Meteorological Administration, Beijing, China*

[b] *Collaborative Innovation Center on Forecast and Evaluation of Meteorological Disasters (CIC-FEMD), Nanjing University of Information Science & Technology, Nanjing, China*

[c] *Climate Research Division, Environment and Climate Change Canada, Toronto, Canada*

*Corresponding author*: Ying Sun, sunying@cma.gov.cn

CAPSULE

The greenhouse gas forcing has increased the likelihood of events like the 2021 wettest September in northern China by ~2-fold, while the anthropogenic aerosols play a relatively minor suppressing role.

## 1. Introduction

The autumn of 2021 was very unusual in northern China (NC). Continuous heavy rainfall hit the region in the September of the year. September is generally dry in in the region with mean total precipitation amount about 64 mm over 1951-2021. The 158.2 mm of total precipitation in September 2021 exceeded normal years by about 4 standard deviations (26 mm). The record rainfall led to high water levels and large water flows along the middle and lower reaches of the Yellow River Basin, resulting in serious flooding and landslides. Some ancient buildings were permanently damaged because of severe flooding (NCHA, 2021). About 6.668 million people and 498,600 hectares of agricultural land were affected, leading to a direct economic loss of about 15.34 billion CNY (MEM, 2021; NCC, 2021). It is thus necessary to explore what caused such an anomalous autumn in NC.

Previous studies have found anthropogenic influence on intensification of heavy precipitation at global scale and in continents like Asia (Zhang et al., 2013; Paik et al., 2020; Dong et al., 2021). In China, several event attribution studies provide evidence of human influence on increased probability or magnitude of heavy precipitation at smaller regional scale such as southeastern China in summer (Burke et al., 2016; Sun et al., 2019) and Beijing City in northern China in winter (Pei et al., 2022). However, a few studies found no clear evidence for the anthropogenic influence in NC (Zhou et al., 2013) or a negative contribution in central western China (Zhang et al., 2020) and southern China (Li et al., 2021). Many factors may have contributed to the different conclusions among the studies, including the event definition (Leach et al., 2020), the framing (Christidis et al., 2018), spatial and temporal contexts of the event (Kirchmeier-Young et al., 2019; Leach et al., 2020), as well as the use of different indicators (Sippel and Otto, 2014; Wehner et al., 2016). Besides the effect of greenhouse gases on heavy precipitation, the anthropogenic aerosols have also been found to possibly reduce the probability of extreme precipitation in the Yangtze River Valley (Zhou et al., 2021). Most previous studies

have focused on the summer precipitation analysis, while few have looked at autumn precipitation. Here we employ a probability-based approach (Stott et al., 2016) to explore the influence of anthropologic forcing as a whole and of the individual forcing such as greenhouse gases and anthropologic aerosols on the 2021-like autumn event in NC.

## 2. Data and methods

We used homogenized station data during 1951–2021 (http://data.cma.cn/) provided by China National Meteorological Information Center (NMIC) to characterize the rainfall in northern China (Red box in Figs. 1a–c, 32.5–42.5°N,110–120°E). Daily precipitation data from 618 stations were selected and averaged onto the grid boxes at 2.5°×2.5°. The regional observation is extracted at the regional means of the area-weighted gridded data first and then normalized (relative to 1961–1990) as percentage anomalies of monthly mean precipitation (MPPA), maxima of 1-day (Rx1day%) and consecutive 5-day (Rx5day%) precipitation. We used simulations by climate models participated in the Coupled Model Intercomparison Project Phase 6 (CMIP6, Eyring et al., 2016) under all anthropogenic and natural forcings combined (ALL), well-mixed greenhouse gas forcing (GHG), anthropogenic aerosol forcing (AA) and natural forcing (NAT), as well as the pre-industrial control simulations(CTL). To avoid giving too much weight to any individual model, we chose the models providing 3 ensemble members under each forcing and we also took the relevant CTL simulations of the same length (more details listed in Tables ES1 and ES2 in the online supplemental material). As 2015–2020 segments of GHG, AA and NAT simulations were driven by the SSP2-4.5 emission scenario (Gillett et al., 2016), the ALL historical simulations (1850–2014) were extended to 2021 with results from the SSP2-4.5 scenario. The simulations were interpolated onto the same grid boxes as the observation using bilinear interpolation. The area-weighted averages of these regridded data were then used to obtain simulated MPPA, Rx1day% and Rx5day% of each ensemble member of the models. Note that for each model, the baseline period of 1961–1990 was constructed from its ensemble mean response to ALL forcing and used for all the simulations in order to keep impacts from the external forcing.

We used risk ratio (RR) to quantify anthropogenic contribution to changes in event probabilities (Stott et al., 2016). For MPPA, the probability of events was calculated using the

method described in Sun et al. (2019) based on the empirical probability formula (Bonsal et al., 2001). For Rx1day% and Rx5day%, a generalized extreme value (GEV) distribution was fitted to the observed and simulated data. The probability of events with equivalent or heavier precipitation than the September 2021 event in the 11-year simulations (2010–2020) under ALL, NAT, GHG, and AA forcings were defined as $P_{ALL}$, $P_{NAT}$, $P_{GHG}$, and $P_{AA}$, respectively. $P_{CTL}$ denoted the occurrence probability of the events that are equal to or exceed the observed magnitude of the 2021-event in all the CTL simulations. The change in probability of a 2021-like event in the factual and counterfactual climates can thus be expressed as $RR_{ALL} = P_{ALL}/P_{NAT}$. Similarly, we used $RR_{GHG} = P_{GHG}/P_{CTL}$ and $RR_{AA} = P_{AA}/P_{CTL}$ to denote the ratio of the probability under only GHG or AA forcing to that without human interference (i.e., at CMIP6-specified pre-industrial level). The 90% confidence interval (90% CI) was obtained by using 1000 bootstrap resampling.

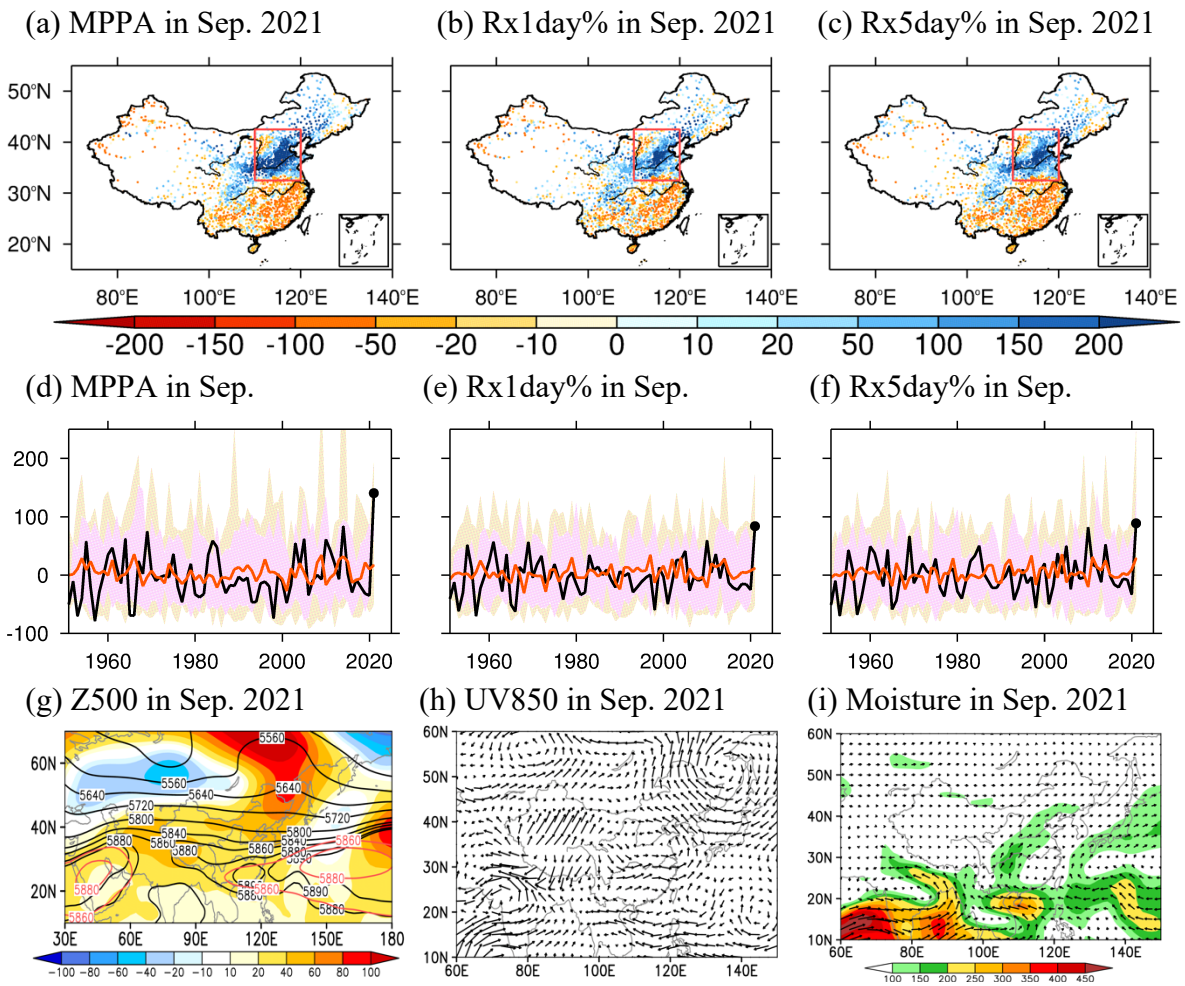

Fig. 1. (a)–(c) Observed MPPA, Rx1day% and Rx5day% in September 2021 over China. Red box marks the study region of northern China. (d)–(f) Regional averaged September MPPA, Rx1day% and Rx5day% in NC during 1951–2021 for observation (black) and model simulations under ALL (red) forcing. The pink and yellow hatchings show the 5–95% and minimum-maximum spreads of ALL simulations, respectively. (g) Geopotential height (contour, gpm) and anomalies (shading, gpm) at 500 hPa. (h) Wind anomalies ($m \cdot s^{-1}$) at 850 hPa. (i) Moisture flux (arrow, $kg \cdot s^{-1} \cdot m^{-1}$) vertically integrated from 1000 hPa to 300 hPa and its divergence (shading, $10^{-5}$ $kg \cdot s^{-1} \cdot m^{-2}$). All anomalies are relative to 1961–1990.

## 3. Results

In September 2021, two thirds of the stations (416 stations) in Northern China experienced more than twice the 1961–1990 averaged MPPA and nearly 40% (235 stations) of the stations reached a new record since 1951 (Fig. 1a). Three stations even received 6 times more precipitation than the 1961–1990 average. The observed MPPA ($MPPA_{OBS}$) of 140.5% in September 2021 is the highest since 1951 (Fig. 1d), expected to recur once every 103 (90% CI: 61–1401) years (Fig. ES1a). Observed Rx1day% and Rx5day% in 2021 show spatial distributions similar to that of the MPPA (Figs. 1b, c), with the highest amount of 83.87% and 88.82% averaged in NC relative to 1961–1990 during 1951–2021, respectively (Figs. 1e, f). Such high values corresponded to a 1-in-334-yr event and a 1-in-167-yr event (Figs. ES1 b, d). All these indicated a record-breaking wet event marked by abnormal mean and extreme rainfall.

The atmospheric circulation and water vapor transport provided favorable background for the persistent rainfall. During September 2021, a stable mid-latitude circulation with two troughs and one ridge (Fig. 1g) was conducive to the formation and maintenance of precipitation systems in northern China. The subtropical high extended westward and southwestly airflow prevailed at the western edge of its lower level, which brought water vapor continuously to the study region, providing abundant water vapor for precipitation (Figs. 1h, i). The similar circulation pattern was also found in autumn of NC in some La Niña years (Yuan and Wang, 2019), which reflects the possible influence from a La Niña event.

The CMIP6 models have comparable standard deviations with the observation and reasonably reproduce the observed distributions of the three variables as their probability distributions were not considered to be statistically different from those of observations' according to the two-sided Kolmogorov-Smirnoff test (Fig. ES1). Note, however, that differences in the far tails of the distribution between the simulation and the observation is

visible. The 2021 observation is very unusual as it is close to or ever higher than 95% of the simulations (Figs. 1d-f).

Using the Bonsal method (2001), the probability of exceeding the 2021 threshold in $MPPA_{OBS}$ is 0.97% ($P_{OBS}$=0.0097). The corresponding probability of a 2021-like event defined by $MPPA_{OBS}$ is 2.1% (0.6%–3.2%) under ALL forcing and 1.7% (0.1–3%) under NAT forcing, which is associated with a 1-in-48-yr (31–167 yr) event and a 1-in-60-yr (33–100 yr) event, respectively (Figs. 2 a, b). Thus, such events are estimated to be more common because of human influence as $RR_{ALL}$ =1.3 (0.1–2.0). Following this process and the same $MPPA_{OBS}$, we estimate the corresponding $RR_{GHG}$ and $RR_{AA}$ to be 2.3 (1.3–3.2) and 0.5 (0.1–1.0), respectively (Figs. 2 c -e).

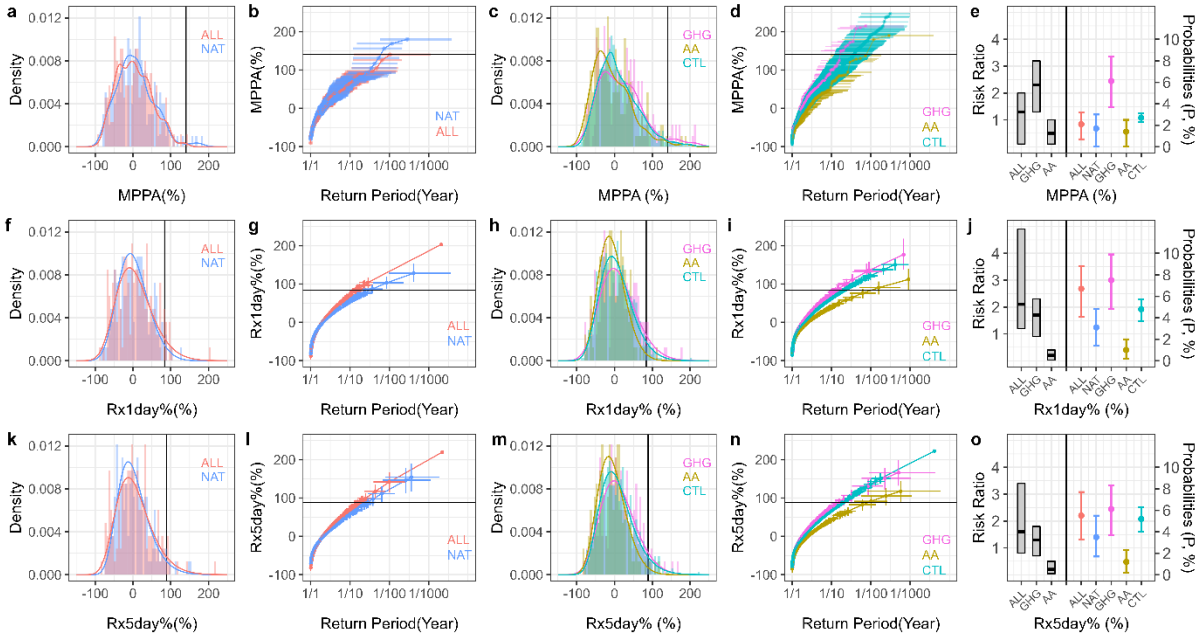


Fig. 2. Attribution results. Fitted distributions, return periods, risk ratios and exceedance probabilities of domain-averaged MPPA by the empirical probability formula (Figs. a–e), and Rx1day% (Figs. f-j) and Rx5day% (Figs. k-o) by GEV distribution in September 2021 over northern China based on ALL (red), NAT (blue), GHG(purple), AA(Orange) and CTL (green) ensembles. Black lines indicate the observed threshold values of the September 2021 event, that is 140.5%, 83.87% and 88.82% for MPPA, Rx1day% and Rx5day%, respectively. Figs. (e)- (o) are best estimates and 90% confidence intervals of risk ratios (left, gray boxes) and exceedance probabilities (right, color bars). The error bars and boxes mark 5–95% uncertainty ranges estimated via the bootstrapping method (N = 1000).

Figs. 2f-o shows the GEV-fitted probability distributions, return periods and risk ratios of Rx1day% and Rx5day% for the 2021-like event under different external forcings. For both indices, the ALL distributions show a relatively lower and wider shape, and a shift to higher amounts as compared to the NAT climate. This indicates an increase in the probability of a 2021-like event in response to anthropogenic forcing. For Rx1day%, the probability higher than the observed threshold (83.87%) is 6.7% (4.1%–8.8%) in ALL and 3.1% (1.4%–4.8%) in NAT. Then $RR_{ALL}$ is estimated as 2.1 (1.2–4.9). Further comparison between forced and unforced experiments shows the influence of different anthropogenic forcings. As compared to the CTL, the GHG is marked by a flatter distribution, shifting rightward to a wetter climate in most cases, while the AA distribution has a narrower shape shifting to a drier world. The estimated $P_{GHG}$, $P_{AA}$ and $P_{CTL}$ indicate that a 1-in-21-yr (17–27) event in CTL becomes a 1-in-13-yr (10–21 yr) event with $RR_{GHG}$=1.7(0.9–2.3) in GHG and a 1-in-100-yr (51–597 yr) event in AA with $RR_{AA}$=0.2 (0.03–0.4). Similarly for Rx5day% (Figs. 2 k-o), we estimate $RR_{ALL}$ =1.6 (0.8–3.4), $RR_{GHG}$ =1.3 (0.6–1.8) and $RR_{AA}$=0.2 (0.04–0.5).

## 4. Conclusions

We estimated the anthropogenic influence on the wettest September in 2021 in northern China. Compared to a climate without human influence, the GHG forcing is estimated to induce about 2-fold increases in the probability of both the monthly mean rainfall and heavy rains for one day and five consecutive days for such events. The anthropogenic aerosol forcing shows decreased contribution, which varies among different aspects of the event. It indicates the dominant role of greenhouse gases and a relatively slight suppressing contribution of the anthropogenic aerosols to the occurrence of a 2021-like event in northern China. The possible physical explanation may include the increasing atmospheric water-holding capacity due to increasing GHGs following the Clausius-Clapeyron relationship, which favors the occurrence of heavy rainfall. The impact of anthropogenic aerosols may be more complex. It has masked the GHG-induced warming by its cooling effect and also affected circulation patterns. The aerosols also can exert negative impacts on the heavy rainfall in northern China by weakening the summer monsoon circulation (Jiang, et al., 2015). Results show that the anthropogenic forcing as a whole has increased the likelihood of a 2021-like event, though evidence for the effect on total precipitation is less robust.

*Acknowledgments.*

This study was supported by the National Natural Science Foundation of China (42025503), National Key R&D Program of China (2018YFA0605604) and Key Innovation Team of China Meteorological Administration "Climate Change Detection, Impact and Response" (CMA2022ZD03).

*Data Availability Statement.*

The following data are available online: the CMIP6 GCM simulations (https://esgf-node.llnl.gov/projects/cmip6/), and the homogenized station data in China (http://data.cma.cn/).

REFERENCES

Bonsal, B. R., Zhang, X., Vincent, L. A., and Hogg, W. D., 2001: Characteristics of daily and extreme temperatures over Canada. *J. Clim.*, **14**, 1959–1976, https://doi.org/10.1175/1520-0442(2001)014<1959:CODAET>2.0.CO;2

Burke, C., Stott, P., Ciavarella, A., and Sun, Y., 2016: Attribution of Extreme Rainfall in Southeast China During May 2015. *Bull. Amer. Meteor. Soc.,* **97**, S92–S96. https://doi.org/10.1175/BAMS-D-16-0144.1.

Christidis, N., Ciavarella, A., and Stott, P. A., 2018: Different Ways of Framing Event Attribution Questions: The Example of Warm and Wet Winters in the United Kingdom Similar to 2015/16. *J. Clim.,* **31**, 4827–4845. https://doi.org/10.1175/JCLI-D-17-0464.1.

Dong, S., Sun, Y., Li, C., Zhang, X., Min, S.-K., and Kim, Y.-H., 2021: Attribution of Extreme Precipitation with Updated Observations and CMIP6 Simulations. *J. Clim.,* **34**, 871–881. https://doi.org/10.1175/JCLI-D-19-1017.1.

Eyring, V., Bony, S., Meehl, G. A., Senior, C. A., Stevens, B., Stouffer, R. J., and Taylor, K. E., 2016: Overview of the coupled model intercomparison project Phase 6 (CMIP6)

198 experimental design and organization. *Geosci. Model Dev.,* **9**: 1937–1958,
199 https://doi.org/10.5194/gmd-9-1937-2016

200 Gillett, N. P., Shiogama, H., Funke, B., Hegerl, G., Knutti, R., Matthes, K., Santer, B. D., Stone,
201 D., and Tebaldi, C., 2016: The Detection and Attribution Model Intercomparison Project
202 (DAMIP v1.0) contribution to CMIP6. *Geosci. Model Dev.,* **9**, 3685–3697.
203 https://doi.org/10.5194/gmd-9-3685-2016

204 Jiang, Y., X.-Q. Yang, and X. Liu., 2015: Seasonality in anthropogenic aerosol effects on East
205 Asian climate simulated with CAM5. *J. Geophys. Res. Atmos.*,**120**,10837–10861,
206 https://doi.org/10.1002/2015JD023451

207 Kirchmeier-Young, M. C., Wan, H., Zhang, X., and Seneviratne, S. I., 2019: Importance of
208 Framing for Extreme Event Attribution: The Role of Spatial and Temporal Scales. *Earth's*
209 *Future*., **7**, 1192–1204. https://doi.org/10.1029/2019EF001253

210 Leach, N. J., Li, S., Sparrow, S., van Oldenborgh, G. J., Lott, F. C., Weisheimer, A., et al., 2020:
211 Anthropogenic Influence on the 2018 Summer Warm Spell in Europe: The Impact of
212 Different Spatio-Temporal Scales. *Bull. Amer. Meteor. Soc.*, **101**, S41–S46.
213 https://doi.org/10.1175/BAMS-D-19-0201.1.

214 Li, R., and Coauthors, 2021: Anthropogenic influences on heavy precipitation during the 2019
215 extremely wet rainy season in southern China. *Bull. Amer. Meteor. Soc.*, **102**, S103–S109,
216 https://doi.org/10.1175/BAMS-D-20-0135.1

217 MEM, 2021: China National Natural Disaster Situation in the First Three Quarters of 2021.
218 Ministry of Emergency Management of the People's Republic of China, accessed 30 October
219 2021, https://www.mem.gov.cn/gk/tjsj/

220 NCC, 2021: China Monthly Climate Bulletin in September 2021. National Climate Center of
221 China Meteorological Administration, 15pp, accessed 30 October 2021, https://cmdp.ncc-
222 cma.net/influ/moni_china.php

223 NCHA, 2021: Take multiple measures to improve the disaster prevention and mitigation
224 capabilities of cultural relics and ancient buildings, National Cultural Heritage

Administration of China, accessed 30 October 2021, http://www.ncha.gov.cn/art/2021/10/13/art_722_171288.html

Paik, S., Min, S., Zhang, X., Donat, M. G., King, A. D., and Sun, Q., 2020: Determining the Anthropogenic Greenhouse Gas Contribution to the Observed Intensification of Extreme Precipitation. *Geophys. Res. Lett.,* **47**, e2019GL086875. https://doi.org/10.1029/2019GL086875.

Pei, L., Yan, Z., Chen, D., and Miao, S., 2022: The Contribution of Human-Induced Atmospheric Circulation Changes to the Record-Breaking Winter Precipitation Event over Beijing in February 2020, *Bull. Amer. Meteor. Soc.*, **103**, S55–S60. https://doi.org/10.1175/BAMS-D-21-0153.1

Sippel, S., and Otto, F. E. L., 2014: Beyond climatological extremes – assessing how the odds of hydrometeorological extreme events in South-East Europe change in a warming climate. *Clim. Change,* **125**, 381–398. https://doi.org/10.1007/s10584-014-1153-9.

Stott, P.A., Christidis, N., Otto, F.E.L., Sun, Y., Vanderlinden, J.-P., van Oldenborgh, G.J., Vautard, R., von Storch, H., Walton, P., Yiou, P. and Zwiers, F.W., 2016: Attribution of extreme weather and climate-related events. *WIREs Clim. Change,* **7**, 23–41. https://doi.org/10.1002/wcc.380

Sun, Y., Dong S., Hu T., Zhang X., and Stott P., 2019: Anthropogenic influence on the heaviest June precipitation in southeastern China since 1961. *Bull. Amer. Meteor. Soc.*, **100**, S79–S83, https://doi.org/10.1175/BAMS-D-18-0114.1.

Wehner, M., Stone, D., Krishnan, H., AchutaRao, K., and Castillo, F., 2016: The Deadly Combination of Heat and Humidity in India and Pakistan in Summer 2015. *Bull. Amer. Meteor. Soc.*, **97**, S81–S86. https://doi.org/10.1175/BAMS-D-60 16-0145.1.

Yuan, C., & Wang, D., 2019: Interdecadal variations in El Niño-Southern oscillation impacts on the autumn precipitation in the eastern China. International Journal of Climatology, **39,** 5316-5326. https://doi.org/10.1002/joc.6156

Zhang, W., and Coauthors, 2020: Anthropogenic influence on 2018 summer persistent heavy rainfall in central western China. *Bull. Amer. Meteor. Soc.*, **101**, S65–S70, https://doi.org/10.1175/BAMS-D-19-0147.1.

Zhang, X., Wan, H., Zwiers, F. W., Hegerl, G. C., and Min, S.-K., 2013: Attributing intensification of precipitation extremes to human influence. *Geophys. Res. Lett.*, **40**, 5252–5257. https://doi.org/10.1002/grl.51010.

Zhou, T., Ren, L. and Zhang, W., 2021: Anthropogenic influence on extreme Meiyu rainfall in 2020 and its future risk. *Sci. China Earth Sci.,* **64**, 1633–1644. https://doi.org/10.1007/s11430-020-9771-8

Zhou, T., Song, F., Lin, R., Chen, X., and Chen, X., 2013: The 2012 north China floods: explaining an extreme rainfall event in the context of a longer-term drying tendency. *Bull. Amer. Meteor. Soc.*, **94**, S49–S52. https://doi.org/10.1175/BAMS-D-13-00085.1